

Predicting trends in atmospheric CO₂ across the Mid-Pleistocene Transition using existing climate archives

Jordan R.W. Martin¹, Joel Pedro^{2,3}, Tessa R. Vance³

¹Institute for Marine and Antarctic Studies, University of Tasmania, Hobart, 7004, Australia

²Australian Antarctic Division, Kingston, 7050, Australia

³Australian Antarctic Program Partnership, Institute for Marine and Antarctic Studies, University of Tasmania, Hobart, 7004, Australia

Correspondence to: Jordan R.W. Martin (jrmartin@utas.edu.au)

Abstract

During the Mid-Pleistocene Transition (MPT), ca. 1200–800 thousand years ago (kya), the Earth's glacial cycles changed from 41 kyr to 100 kyr periodicity. The emergence of this longer ice-age periodicity was accompanied by higher global ice volume in glacial periods and lower global ice volume in interglacial periods. Since there is no known change in external orbital forcing across the MPT, it is generally agreed that the cause of this transition is internal to the earth system. Resolving the climate, ~~carbon cycle~~ ~~and~~ ~~–~~ cryosphere ~~dynamics~~ processes responsible for the MPT remains a major challenge in earth and palaeoclimate science. To address this challenge, the international ice core community has ~~prioritised~~ ~~prioritized~~ recovery of an ice core record spanning the MPT interval. ~~The data from such 'oldest ice' projects are still several years away.~~ Here we present results from a simple ~~generalised~~ ~~generalized~~ least squares model that predicts atmospheric CO₂ out to 1.5 Myr. Our prediction utilises existing records of atmospheric carbon dioxide (CO₂) from Antarctic ice cores spanning the past 800 kyr along with the existing LR04 benthic $\delta^{18}\text{O}_{\text{calcite}}$ stack (Lisiecki & Raymo, 2005; ~~hereafter 'benthic $\delta^{18}\text{O}$ stack'~~) from marine sediment cores. Our predictions assume that the relationship between CO₂ and benthic $\delta^{18}\text{O}_{\text{calcite}}$ over the past 800 thousand years can be extended over the last one and a half million years. The implicit null hypothesis is that there has been no fundamental change in feedbacks between atmospheric CO₂ and the climate parameters represented by benthic $\delta^{18}\text{O}_{\text{calcite}}$, global ice volume and ocean temperature.

We test the GLS-model predicted CO₂ concentrations against observed blue ice CO₂ concentrations, $\delta^{11}\text{B}$ -based CO₂ reconstructions from marine sediment cores and $\delta^{13}\text{C}$ of leaf-wax based CO₂ reconstructions (Higgins *et al.*, Yan *et al.*, 2019 and Yamamoto *et al.*, 2022). We show that there is not clear evidence from the existing blue ice or proxy CO₂ data to reject our predictions nor our associated null-hypothesis. A definitive test and/or rejection of the null hypothesis may be provided following recovery and analysis of continuous oldest ice core records from Antarctica, which is still several years away. The record presented here should provide a useful comparison for the oldest ice core records and opportunity to provide further constraints on the processes involved in the MPT.

39
40
41
42
43
44
45
46
47
48
49
50
51
52
53
54
55
56
57
58
59
60
61
62
63
64
65
66
67
68
69
70
71
72
73
74
75
76
77
78

1 Introduction

Ice core records from Antarctica provide comprehensive and continuous records of many climate parameters over the last 800 thousand years, e.g. from the Vostok (Petit *et al.*, 1999) and European Project for Ice Coring in Antarctica's Dome-C (EDC) ice cores (Jouzel *et al.*, 2007). One of the major challenges in climate science lies beyond the current threshold of the ice core record. The Mid-Pleistocene Transition (MPT) spans from ca. 1200–800 thousand years ago (kya) (Chalk *et al.*, 2017) and is characterised by a change from regularly paced 40 thousand year (kyr) glacial cycles with thinner glacial ice sheets to quasi-periodic 100 kyr glacial cycles in which ice sheets are more persistent and thicker (Clark *et al.*, 2006, Chalk *et al.*, 2017). To resolve the forcings and feedbacks involved in this transition, multiple nations are targeting recovery of continuous ice cores spanning the MPT under the framework of the International Partnerships in Ice Core Science (IPICS) oldest ice core challenge (IPICS, 2020).

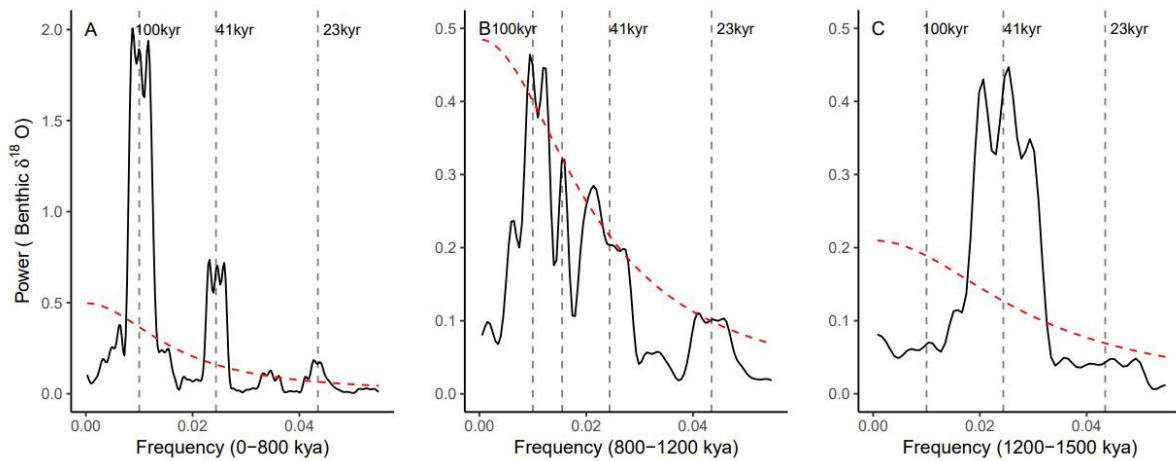
The purpose of the current study is to make a simple prediction of atmospheric CO₂ across the MPT. Cross-comparison of our and other predicted CO₂ records against observed MPT CO₂ data will aid in testing competing hypotheses on the cause of the transition, in particular the role of carbon cycle changes.

The MPT occurred in the absence of any changes to orbital insolation forcing, therefore, the mechanisms behind the MPT must be internal to the earth system (Raymo, 1997; Ruddiman *et al.*, 1989). Multiple hypotheses have been put forward to explain the transition. A common element in many of these, is internal climate/earth system changes which allow for the development of thicker, more extensive ice sheets that could endure insolation peaks corresponding to the 23 kyr precession and 41 kyr obliquity cycles, i.e., an increase in the threshold for deglaciation and altered sensitivity to orbital forcings (Tzedakis *et al.*, 2017; McClymont *et al.*, 2013, Tzedakis *et al.*, 2017;). Indeed, the skipped obliquity cycle hypothesis, proposes that 100 kyr signal seen in spectral analysis of the post-MPT benthic $\delta^{18}\text{O}$ stack (e.g. Fig 1A) may be comprised of alternating 80 and 120-kyr signals, i.e. in which the intervening obliquity cycles are skipped. Among the prominent hypotheses to explain an increased threshold for deglaciation are the following three.

- 1) A long-term decrease in radiative forcing due to a secular reduction in atmospheric CO₂ across the transition (e.g. Berger *et al.*, Hönisch *et al.*, 2009; 1999, Raymo *et al.*, 1988). According to this view, reduced radiative forcing drives the formation of larger and more stable ice sheets.
- 2) Progressive removal of sub-glacial regolith during the 41 kyr glacial cycles. Clark & Pollard (1998) proposed that ice sheet basal sliding prior to the MPT was enhanced by the presence of a low-friction sedimentary regolith layer between the Laurentide ice sheet and the crystalline bedrock. According to this view, progressive removal of this sedimentary layer then favoured the development of larger and more persistent post-MPT ice sheets.
- 3) Phase-locking of the Northern and Southern Hemisphere ice sheets. In frequency spectra of the global marine benthic $\delta^{18}\text{O}$ record (Fig. 1) there is no evidence of the precession (23 kyr) component of northern hemisphere insolation prior to the MPT; the spectra is dominated by the obliquity (41 kyr) component (Fig. 1C). Emergence of significant precession and 100 kyr eccentricity-signals occurs across the MPT (Fig. 1B), and all three components are clearly present after the MPT (Fig. 1A). Raymo

79 *et al.* (2006) suggested that precession-paced changes in northern and southern hemisphere ice volumes
 80 may have occurred prior to the MPT, but are cancelled due to out-of-phase ice volume changes
 81 between the two hemispheres (Raymo & Huybers, 2008). According to this view, during the MPT the
 82 precession-paced changes to fall into phase between the two hemispheres, such that the precession
 83 signal emerges (Raymo *et al.*, 2006). In this view the global synchronization of ice volume drives the
 84 formation of larger and more stable ice sheets.

85
 86 These hypotheses are not mutually exclusive. For a recent review on the cause of the MPT see Berends *et al.*
 87 (2021a).



89
 90
 91 **Figure 1: Thomson Multi-taper Method (MTM) spectral analysis representing relative power of signal periodicity for:**
 92 **A) Benthic $\delta^{18}\text{O}$ stack after (0–800 kya) the Mid-Pleistocene Transition (MPT); B) Benthic $\delta^{18}\text{O}$ across the MPT (800–**
 93 **1200 kya); C) Benthic $\delta^{18}\text{O}$ prior to the onset of the MPT (1200 kya–1500 kya). Each with a robust AR (1) 95 %**
 94 **Confidence interval (red dashed line). Benthic $\delta^{18}\text{O}$ stack data from Lisiecki and Raymo (2005).**

95
 96 For a long-term decrease in radiative forcing by atmospheric CO_2 to be the cause of the MPT, the reduction in
 97 CO_2 would be expected in both glacial and interglacial stages (Chalk *et al.*, 2017). However, low resolution
 98 boron-isotope-based CO_2 reconstructions by Hönisch *et al.*, (2009), and Chalk *et al.*, (2017) suggest that glacial-
 99 stage CO_2 drawdown occurred over the MPT in the absence of interglacial CO_2 drawdown. Glacial-stage CO_2
 100 draw-down across the MPT may be a positive climate-carbon cycle feedback to changes in ice sheet dynamics,
 101 including CO_2 drawdown by enhanced iron fertilisation of the Southern Ocean in response to exposed
 102 continental shelves due to lower sea level, as well as planetary drying associated with colder climate conditions
 103 (Chalk *et al.*, 2017). Colder glacial temperatures that enhance the solubility of CO_2 in the oceans, and reduced
 104 abyssal ocean ventilation has also been implicated in enhanced glacial-stage ocean storage of CO_2 (McClymont
 105 *et al.*, 2013; Hasenfratz *et al.*, 2019).

106
 107 Testing of hypotheses on the cause of the MPT is currently limited by the lack of a continuous ice core that
 108 spans its duration. The International Partnership in Ice Core Sciences (IPICS) has nominated recovery of such a
 109 record as a key priority in ice core research (IPICS, 2020). Multiple national and international projects have

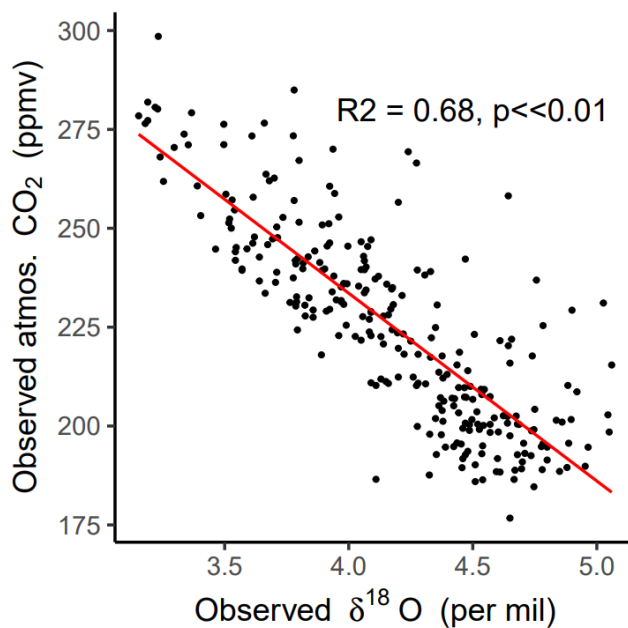
110 commenced, or are soon to commence, drilling for ‘oldest ice’ (see e.g. Shugi, 2022). In this project, we take
111 inspiration from the “EPICA Challenge” in which the paleoclimate and modeling community was challenged to
112 predict the global atmospheric carbon dioxide and methane concentrations from 800–400 kya based on the
113 existing 400 kyr Vostok ice core record (Wolff *et al.*, 2004). Here, we use a generalised least squares (GLS)
114 model trained on continuous climate archives to predict a CO₂ record out to 1.5 Mya. We utilise two primary
115 data sets for the GLS model: the existing 800 kyr ice core composite record of atmospheric CO₂ (Bereiter *et al.*,
116 2015) and the LR04 benthic stack of 52 globally-distributed records of the ¹⁸O to ¹⁶O ratio of fossil benthic
117 foraminifera calcite (hereafter referred to as the LR04 δ¹⁸O benthic stack). The δ¹⁸O ratios in the LR04 benthic
118 stack are governed [primarily](#) by [deep](#) ocean temperature and global ice volume at the time the foraminifera
119 lived, with higher values indicating both increased ice volume and a colder climate. [The relationship between](#)
120 [the ice volume and ocean temperature components contributing to the δ¹⁸O benthic stack are not linear.](#)
121 [Separating the two signals remains challenging and has been attempted elsewhere using a range of approaches](#)
122 [from comparison with paired deep ocean temperature proxies \(Elderfield *et al.*, 2012\), inverse modelling](#)
123 [\(Berends *et al.*, 2021b\) and spectral analysis \(e.g. Huybers and Wunsch, 2009\).](#)

124
125 Fig. 2 shows a scatter-plot of the LR04 δ¹⁸O benthic stack versus observed ice core CO₂ over the past 800 kyr.
126 Both data sets are binned to equivalent 3-kyr time steps (Methods). The Pearson’s correlation coefficient (r)
127 between the data sets is -0.82 (p < 0.05) indicating that ~68% of the variance in observed CO₂ is shared with the
128 LR04 δ¹⁸O benthic stack. This strong relationship provides an initial rationale for using the LR04 δ¹⁸O benthic
129 stack as an input parameter to predict CO₂ beyond 800 kyr. Mechanistically, multiple processes are expected to
130 contribute to the shared variance. A first order factor is the dependency of CO₂ solubility on ocean temperature
131 (e.g. Millero, 1995). From the simple solubility perspective, colder climate states with increased ice volume and
132 colder ocean temperatures will drive increased ocean uptake of CO₂ (Berends *et al.*, 2021a). However, the
133 solubility effect only accounts for a portion of observed glacial CO₂ drawdown (Archer *et al.*, 2000). Multiple
134 additional contributors to the shared variance are proposed in the literature. These include (not exhaustively),
135 direct radiative forcing of ice volume changes by CO₂ (e.g. Shackleton *et al.*, 1985); the impact of ice
136 volume/sea level changes on atmospheric CO₂ via ocean productivity and carbonate chemistry changes (e.g.
137 Broecker, 1982; Archer *et al.*, 2000; Ushie and Matsumoto, 2012); CO₂ drawdown during periods of high ice
138 volume by increased iron ~~fertilisation~~[fertilization](#) (e.g. Röthlisberger *et al.*, 2004; Martinez-Garcia *et al.*, 2014)
139 and enhanced sea ice extent during periods of high ice volume capping the ventilation of CO₂ from the ocean
140 interior at high latitudes (Stephens and Keeling, 2000).

141
142 A quantitative separation and attribution of the processes linking global ice volume, ocean temperature and
143 atmospheric CO₂ on millennial to orbital timescales is not currently available (e.g. Archer *et al.*, 2000; Sigman
144 *et al.*, 2010; Gottschalk *et al.*, 2019) and will not be attempted here. Rather, we make the simple assumption that
145 the relationships between the LR04 benthic δ¹⁸O stack and CO₂ can be extended beyond 800 kya and use
146 [generalised least squares \(GLS\)](#) regression modelling between benthic δ¹⁸O and CO₂ to make a predictions of
147 CO₂ spanning 800–1500 kya. The deliberately simple implicit assumption, and null hypothesis, is that there is
148 no change to the feedback processes linking benthic δ¹⁸O and CO₂ before and after the MPT.

149

150 [This approach differs to previous more complex model studies that have attempted to reconstruct CO₂ using the](#)
151 [LR04 benthic δ¹⁸O stack as an input variable \(van de Wal, 2011; Stap et al., 2016, Berends et al., 2021b\). The](#)
152 [latter studies use an inverse forward modelling approach, in which climate and ice sheet models of various](#)
153 [complexities are used to capture physical relations between CO₂, global temperature and ice volume. For](#)
154 [example, in Berends et al., 2021b the offset between modelled and observed benthic δ¹⁸O is used to calculate a](#)
155 [value for atmospheric CO₂ that is iterated back to the inverse model. The CO₂ record which minimises the](#)
156 [difference between the modelled and observed benthic stack is then taken as an estimate of how atmospheric](#)
157 [CO₂ may have evolved to force coupled climate, deep ocean temperature and land ice volume changes that](#)
158 [reproduce the observed benthic δ¹⁸O signal. Accuracy of the reconstructions in the inverse modelling approach](#)
159 [depends on the ability of the climate and ice sheet models used to capture the correct climate dynamics across](#)
160 [the MPT. Our GLS method is a simpler statistical approach, designed with the specific null hypothesis in mind,](#)
161 [that does not attempt to simulate the physics linking benthic δ¹⁸O signal, land ice volume, global temperature](#)
162 [and CO₂. A range of approaches to reconstructing CO₂ have been called for and are of value in the context of](#)
163 [forthcoming continuous ice core records across the MPT from oldest ice projects currently underway in](#)
164 [Antarctica \[IPICS 2020\].](#)



168 **Figure 2: Scatter plot of the composite observed atmospheric CO₂ record (Bereiter *et al.*, 2015) against**
169 **the LR04 benthic stack of marine δ¹⁸O records (Lisiecki & Raymo, 2005). Red line is a linear line of best**
170 **fit ($R^2 = 0.68$; $p < 0.05$).**

171

172

173 To test ~~the-our~~ null hypothesis, in advance of the recovery of a continuous ice core, we compare our predicted
174 CO₂ record to two sets of low-resolution ice core data that exist outside the current 800 kyr observed CO₂.

175 These data come from direct CO₂ measurements from ancient “blue ice” from the Allan Hills in East Antarctica

176 (hereafter referred to as BI-CO₂) from ca. 1 Mya (Higgins *et al.*, 2015) and 1.5 Mya (Yan *et al.*, 2022). We use
177 the term blue ice to describe deep, ancient glacial ice that has been brought nearer to the surface of an ice sheet
178 by ice flow. Blue ice is sampled by cutting trenches or shallow drilling of up to several hundred meters (e.g.
179 Higgins *et al.*, 2015). The vertical migration of blue ice is associated with high deformation making the ice
180 samples stratigraphically complex and hard to date (Higgins *et al.*, 2015). As a result, blue ice records alone do
181 not provide a continuous CO₂ record across the MPT. [In the Discussion, w](#)We also compare our predicted
182 record to existing proxy-CO₂ reconstructions from boron-isotope analysis of benthic foraminifera in marine
183 sediment records (Chalk, *et al.*, 2017; Dyez *et al.*, 2018; Guillermic *et al.*, 2022), leaf wax δ¹³C carbon isotope
184 ratios (Yamamoto *et al.*, 2022) and predictions from previous models of various complexities (van de Wal *et al.*,
185 2011; Willeit *et al.* 2019; [Berends *et al.* \(2021ba\)](#)). We conclude with discussion of the implications of our
186 results and data-comparisons for the understanding MPT dynamics.

187
188

189 **2 Methods**

190 ~~We use a generalised least squares (GLS) model to predict atmospheric CO₂ from the LR04 benthic δ¹⁸O stack~~
191 ~~(Fig. 3A and B). We apply an AR(1) correlation factor to account for autocorrelation in the data. The AR(1)~~
192 ~~correlation factor yielded the lowest Akaike information criterion (AIC) value from a test of multiple correlation~~
193 ~~factors.~~

194

195 [We use a generalised least squares \(GLS\) model with an auto-regressive \(AR\) factor 1 to predict atmospheric CO₂](#)
196 [from the LR04 benthic δ¹⁸O stack \(Fig. 3A and B\). We use GLS because the assumptions of ordinary least squares](#)
197 [\(OLS\) are violated by the presence of autocorrelation and heteroskedasticity in the regression errors. We selected](#)
198 [the AR\(1\) correlation factor as it yielded the lowest Akaike information criterion \(AIC\) value from a test of](#)
199 [multiple correlation factors. The AR\(1\) process assumes and accounts for dependence of error at a given point in](#)
200 [time on the previous error term. In practise this makes the model assumptions more realistic and improves](#)
201 [parameter estimation where, as in the climate system, observations are dependent on past values.](#)

202

203 To obtain common time steps and resolution between the predictor (LR04 benthic δ¹⁸O stack) and response
204 (CO₂) variables, we re-grid the LR04 benthic stack and Bereiter *et al.*, (2015) CO₂ data into time bins with a
205 resolution of 3-kyr. The GLS regression model was [then](#) applied over the 0–800 kyr range of the predictor and
206 response variables as follows:

207

$$208 \quad CO_2 = 33.37 \times \delta^{18}O + 365.15, \text{ autoregressive (AR) factor: } 1$$

209

210 Based on the regression model, the δ¹⁸O values of the LR04 Benthic Stack from 800 – 1500 kya were used to
211 predict CO₂ concentration over this range (hereafter referred to as PRED-CO₂). ~~To estimate the GLS model~~
212 ~~uncertainty and sensitivity we took a bootstrap approach, selecting a random 50% subset of our data and re-~~
213 ~~running the model 1000 times to determine 95% confidence intervals for the predictions. To gauge the GLS~~
214 ~~model stability we took a bootstrap approach, selecting a random 50% subset of our data (with replacement) and~~
215 ~~re-running the model 1000 times to determine 95% confidence intervals for the predictions. While the GLS~~
216 ~~method itself addresses autocorrelation, the bootstrap method introduces variability such that each iteration of~~

217 [the model has different combinations of the original data points \(including repeated ones\), this variability helps](#)
218 [in assessing the robustness and sensitivity of the model e.g. to variable data and dating uncertainty.](#)

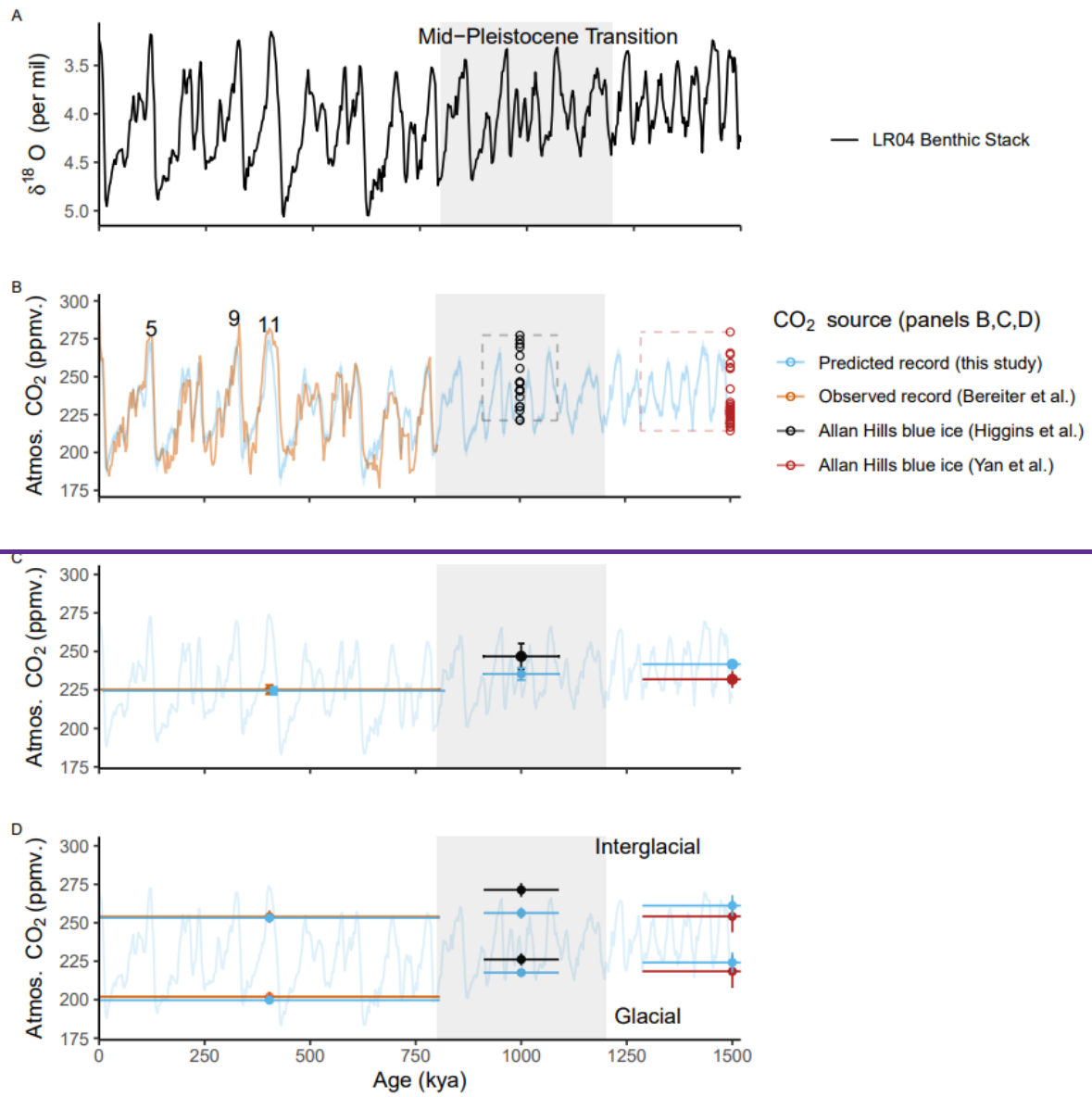
219
220 Uncertainties in the independent age scales of both the LR04 stack and the compiled CO₂ record are inherited by
221 our GLS model and its predictions. The LR04 stack includes 57 globally-distributed benthic δ¹⁸O sediment core
222 records. The age models for these cores are independently constructed from the average sedimentation rates of
223 each core, assuming global sedimentation rates have remained relatively stable, and with tuning to a simple ice
224 model based on 21 June insolation at 65°N (Lisiecki & Raymo, 2005). The authors estimate uncertainty of 6 kyr
225 from 1.5 – 1.0 Mya and 4 kyr from 1 – 0 Mya (Lisiecki & Raymo, 2005). The observed CO₂ composite ice core
226 record for the past 800 kya (Bereiter *et al.*, 2015) uses six independent dating methods for various core locations
227 both spatially across Antarctica, and stratigraphically for different sections of the same core. The age uncertainty
228 in the gas timescale has a median over the 0 – 800 kya interval of 2 kyr, but individual uncertainties can reach
229 up to 5 kyr (Veres *et al.* 2013; Bazin *et al.*, 2013). The relative age uncertainties between these input variables
230 may diminish the regression or in some instances lead to spurious correlation. However, we expect any such
231 effects are minor on the basis that our predictions show little sensitivity ([median, 2σ, 5.78 ppm](#)) (~~median ##~~
232 ~~ppm~~) to the bootstrap analysis [with 1000 iterations of re-computing the regression after removing a randomly](#)
233 [chosen 50% of data for each iteration of the model](#) (see Fig. 3B, C and Discussion).

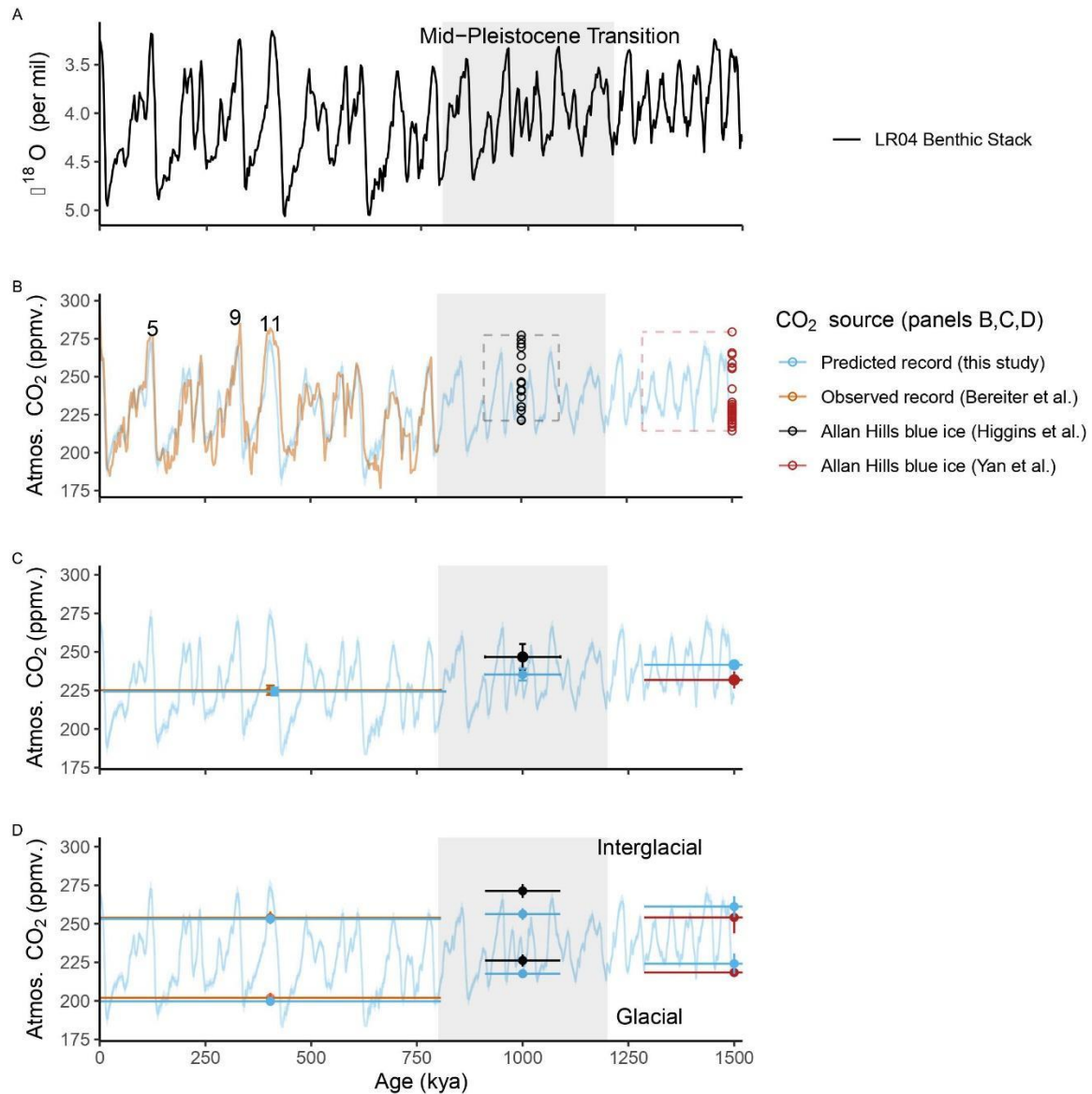
234 235 **3 Results**

236 Fig. 3B shows the time series of our LR04 benthic δ¹⁸O stack-based GLS model predictions of atmospheric CO₂
237 (PRED-CO₂) over the past 800 kyr, in comparison to the observed ice core CO₂ record from Bereiter *et al.*,
238 (2015). The correlation coefficient (R^2) between the predicted and observed records is 0.68 ($p \ll 0.01$). Our
239 PRED-CO₂ record out to 1.5 Mya [with shaded 95% CIs from the bootstrap analysis](#) is also shown, overlain with
240 observed Allan Hills blue ice CO₂ (BI-CO₂) datasets of age 1000 ± 89 kya (Higgins *et al.*, 2015) and $1.5 \text{ Mya} \pm$
241 213 kyr (Yan *et al.*, 2022).

242
243 We evaluate the PRED-CO₂ record against the observed CO₂ data according to criteria of mean concentrations
244 across the common intervals, and mean concentrations in the glacial and interglacial subsets of the data. First,
245 the mean CO₂ concentration over the common intervals (Fig 3C). From 0–800 kya the mean concentration in
246 observed (Bereiter *et al.*, 2015) and PRED-CO₂ data are in close agreement (225.2 ± 3.03 ppm versus the
247 predicted 225.1 ± 2.5 ppm respectively; uncertainties are 95% confidence intervals, i.e. 1.96σ). In the 1000 ± 89
248 kya interval (i.e. averaged across the age uncertainty of the Higgins (2015) blue ice data) the BI-CO₂
249 concentration is ~ 11 ppm higher than PRED-CO₂ (246.7 ± 8.4 ppm versus the predicted 235.5 ± 3.9 ppm), this
250 difference is not significant at the 95% confidence level. For the $1.5 \text{ Mya} \pm 213$ kyr interval, the mean BI-CO₂
251 concentration is ~ 10 ppm lower than PRED-CO₂ (231.9 ± 5.6 ppm versus the predicted 241.7 ± 2.5 ppm),
252 which is marginally significant at the 95% level. Comparisons of mean levels across intervals spanning multiple
253 glacial and interglacial cycles may be ~~biased~~ **biased** if (as is likely) the blue ice data is not sampling glacial and
254 interglacial values with the same uniformity as a continuous record.

256 To address this, we define the glacial and interglacial thresholds of PRED-CO₂ to be respectively the lower and
257 upper 25th percentiles of the LR04 δ¹⁸O predictor variable (following Chalk *et al.*, 2017). Filtering the observed
258 (Bereiter *et al.*, 2015) CO₂ record and our predicted CO₂ record according to these definitions we find a very
259 close match for glacial (202.0 ± 3.2 versus the predicted 199.7 ± 1.7 ppm) and interglacial intervals (253.9 ± 4.1
260 ppm versus the predicted 253.1 ± 2.3 ppm), over the past 800 kya (see Fig. 3D). For blue ice (BI-CO₂) data, a
261 corresponding LR04 isotope signal could not be confidently applied to the measured CO₂ concentration due to
262 the uncertainties associated with blue ice [datingaging](#); therefore, we defined the glacial and interglacial
263 thresholds of blue ice data according to the top (interglacial) and bottom (glacial) 25th percentiles of actual CO₂.
264 Applying this to the 1000 ± 89 kya interval finds that observed BI-CO₂ data is ~ 9 ppm higher than PRED-CO₂
265 during the glacial stages (226.2 ± 4.0 ppm versus the predicted 217.6 ± 2.3 ppm) and ~ 15 ppm higher than
266 PRED-CO₂ during the interglacial stages (271.3 ± 4.5 versus the predicted 256.3 ± 3.8 ppm). These differences
267 are significant with respect to the constrained uncertainties. In contrast, during the $1.5 \text{ Mya} \pm 213 \text{ kyr}$ interval,
268 the mean BI- CO₂ concentration is not significantly different to PRED-CO₂ in either glacial (217.6 ± 2.3 versus
269 the predicted 224.2 ± 6.6 ppm) or interglacial stages (256.3 ± 3.8 versus the predicted 261.1 ± 6.3 ppm). These
270 comparisons, particularly the agreement at 1.5 Myr, indicate that PRED-CO₂ is not drifting systematically away
271 from the existing observed BI-CO₂ data. In our view the disagreement at 1.0 Myr, where BI-CO₂ is elevated
272 with respect to PRED-CO₂, does not give sufficient cause to reject the GLS model, it could of course be a
273 failing in the model and/or could be due to potential biases in the blue ice data, for example elevated CO₂
274 concentrations due to in-situ CO₂ production in blue ice (see Discussion).





276

277 **Figure 3: A) The LR04 Benthic Stack of 57 globally distributed $\delta^{18}\text{O}$ records (Lisiecki & Raymo, 2005).**
 278 **B) Comparison of our PRED-CO₂ (ppm) record to the current continuous composite record (0–800 kya);**
 279 **and to direct CO₂ measurements from Allan Hills blue ice cores (BI-CO₂) ca. 1 Mya (± 89 kyr) (Higgins *et***
 280 ***al.*, 2015) and ca. 1.5 Mya (± 213 kyr) (Yan *et al.*, 2022). Age uncertainty boundaries for the BI-CO₂ data**
 281 **are represented by dashed box boundaries. Marine isotope stages 5, 9, and 11 are numbered on the plot**
 282 **according to Lisiecki & Raymo (2005). [Blue shading around PRED-CO₂ is the 95% CI from bootstrap](#)**
 283 **[analysis.](#) C) Mean concentrations of the PRED-CO₂ and observed composite CO₂ records over the range**
 284 **of the observed composite record (offset for clarity), and the mean concentrations of the PRED-CO₂ and**
 285 **BI-CO₂ data at 1 Mya and again at 1.5 Mya averaged over the age uncertainty range of each BI-CO₂ data**
 286 **set. D) As for C) however filtered by the upper and lower 25th and 75th percentiles to estimate glacial and**
 287 **interglacial periods.**

288

289 We now consider long-term trends in interglacial and (separately) glacial CO₂ levels across the past 1.5 Myr in
 290 PRED-CO₂ and in the existing ice core CO₂ data. For PRED-CO₂ there is no significant difference between CO₂

291 concentrations in the interglacial stages of the $1.5 \text{ Mya} \pm 213 \text{ kya}$, $1000 \pm 89 \text{ kya}$ and $0\text{--}800 \text{ kya}$ windows (Fig 4
292 D, blue bars). In the ice core observations, interglacial levels at 1.5 Mya in BI-CO₂ are also within the
293 uncertainties of those in the $0\text{--}800 \text{ kya}$ interval. Notably, the BI-CO₂ concentrations in the $1000 \pm 89 \text{ kya}$
294 interval appear elevated with respect to the $0\text{--}800 \text{ kyr}$ and $1.5 \text{ Mya} \pm 213 \text{ kya}$ intervals, however this elevated
295 (ca. 271 ppm) level is consistent with the observed interglacial CO₂ concentration during interglacials 5, 9 and
296 11 (Fig 3B). Overall, there is no indication in the observed ice core CO₂ data or in PRED-CO₂ for a long-term
297 trend in *interglacial* CO₂ levels across the past 1.5 Myr.

298

299 In comparison, there are significant declines in glacial CO₂ levels across the MPT in PRED-CO₂ and the
300 observed ice core data. For PRED-CO₂, glacial CO₂ concentrations are not significantly different during the 1.5
301 $\text{Mya} \pm 213 \text{ kya}$ and $1000 \pm 89 \text{ kya}$ windows. However, across the MPT, PRED-CO₂ glacial concentrations drop
302 by $\sim 18 \text{ ppm}$. This pattern is consistent with the observed data, where glacial CO₂ levels are also not significantly
303 different between the $1.5 \text{ Mya} \pm 213 \text{ kya}$ and $1000 \pm 89 \text{ kya}$ windows (217.6 ± 2.3 and $226.2 \pm 4.0 \text{ ppm}$,
304 respectively) and then fall by 24 ppm to the $0\text{--}800 \text{ kyr}$ observed glacial mean of $202.0 \pm 3.2 \text{ ppm}$. Glacial-stage
305 draw-down of CO₂ across the MPT in the absence of interglacial draw-down is consistent with previous
306 observations based on the boron-isotope-based CO₂ reconstructions (e.g., Chalk *et al.*, 2017; Hönisch *et al.*,
307 2009 and see Discussion). In the following section we also compare PRED-CO₂ data to boron-isotope-based and
308 other CO₂ proxy records covering the 0 to 1.5 Myr interval.

309

310 **4 Discussion**

311 Our objective with this manuscript was to generate the simplest reasonable model to predict CO₂ from the LR04
312 $\delta^{18}\text{O}$ benthic stack and to test the predictions against available observations. It is possible that the fit between
313 observed and our predicted CO₂ data could be further improved using a non-linear approach. However, we
314 refrain from a non-linear approach for several key reasons. First, a scatter plot of the LR04 $\delta^{18}\text{O}$ benthic stack
315 versus observed ice core CO₂ over the past 800 kyr yields a Pearson's correlation coefficient (R) of -0.82 (Fig.
316 2), indicating that $\sim 68\%$ of the variance in observed CO₂ is shared with the benthic stack. This is similar to that
317 reported in ; this is supported by ordinary linear least-squares modelling regression ($R^2=0.70$) by Berends *et al.*
318 (2021ba). Importantly, there is no evidence in this scatter plot for departure from the linear relationship at high
319 or low CO₂ or benthic $\delta^{18}\text{O}$ levels. Second, following the approach of Chalk *et al.*, 2017 and interpreting the
320 upper 25th percentile of CO₂ data as representing mean interglacial stage CO₂ and the lower 25th percentile of
321 CO₂ data as representing mean glacial stages CO₂ levels, we see that our predicted interglacial mean value for
322 the past 800 kyr ($253.1 \pm 2.3 \text{ ppm}$) closely overlaps with the observed interglacial mean value ($253.9 \pm 4.1 \text{ ppm}$)
323 and similarly, the predicted glacial stage mean ($199.7 \pm 1.7 \text{ ppm}$) closely overlaps with the observed glacial
324 stage mean ($202.0 \pm 3.2 \text{ ppm}$). Third, the predictions are remarkably insensitive to bootstrap analysis in which
325 50 % of that data are omitted with each iteration of the GLS model (~~Fig 1~~). Such insensitivity to the bootstrap
326 analysis and accurate prediction of glacial *and* interglacial state CO₂ values would be unlikely in the case of
327 major non-linear dependencies between the LR04 predictor and CO₂ response variables. Fourth, non-linear
328 approaches would risk generating an improved fit due to statistical artefacts that do not meaningfully relate to
329 any dependence between benthic $\delta^{18}\text{O}$ and CO₂. Finally, the specific causes and sources and sinks involved in
330 glacial to interglacial and millennial-scale CO₂ variations still remain poorly constrained (e.g. Archer *et al.*,

331 2000; Sigman *et al.*, 2010; Gottschalk *et al.*, 2019). Given this process-uncertainty, the GLS model fits our
332 criteria of the simplest reasonable model. Further, the use of benthic $\delta^{18}\text{O}$ to predict atmospheric CO_2 has
333 precedence; in response to the EPICA challenge (Wolff *et al.*, 2004); N. Shackleton ~~used $\delta^{18}\text{O}$ this method to~~
334 ~~predicted~~ atmospheric CO_2 out to 800 kyr, ~~based on a number of benthic $\delta^{18}\text{O}$ records from the East Pacific~~
335 ~~(Wolff, 2005). Furthermore, I inverse modelling of CO_2 forced by the LR04 benthic stack has~~ ~~been~~
336 ~~undertaken by van de Wal *et al.* (2011), and further expanded by Berends *et al.* (2021a) who utilised a simple~~
337 ~~least squares (LS) rather than a GLS regression, and van de Wal *et al.* (2011).~~

338

339 There are several caveats with blue ice data that may affect its use to evaluate our GLS model predictions. The
340 blue ice data may have been subject to diffusional smoothing of CO_2 (e.g. Yan *et al.*, 2019), which would act in
341 the direction of elevating the (lower 25th percentile) assumed glacial concentrations above the glacial
342 atmospheric values and reducing the (upper 25th percentile) assumed interglacial concentrations. There is also
343 the potential for artificially elevated CO_2 concentrations in blue ice due in-situ respiration of CO_2 due to
344 microbial activity in detrital matter. Respiration effects are screened for by measurements of $\delta^{13}\text{C}$ of CO_2 ,
345 however it is difficult to demonstrate that all samples are unaffected (Yan *et al.*, 2019). These uncertainties
346 support our argument that the GLS-model predictions are not rejected by the available observed BI- CO_2 data.

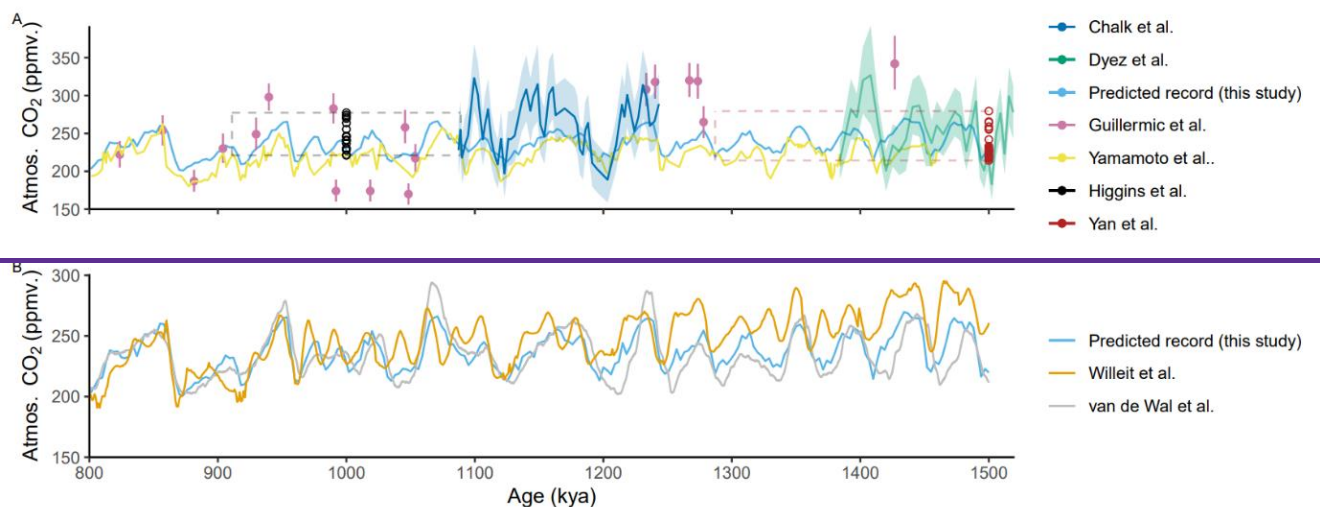
347

348 We consider the BI- CO_2 data to provide the most reliable measurements of CO_2 concentration, in the absence of
349 a continuous ice core record across the MPT. However, further comparison of our CO_2 predictions can also be
350 made against CO_2 proxy data from non-ice core archives (Fig 4A). We consider here $\delta^{11}\text{B}$ -based atmospheric
351 CO_2 reconstructions (Chalk *et al.*, 2017, Dyez *et al.* 2018 and Guillermic *et al.* 2022) and a recent atmospheric
352 CO_2 reconstruction from $\delta^{13}\text{C}$ of leaf wax (Yamamoto *et al.*, 2022). The continuous $\delta^{11}\text{B}$ -based reconstructions
353 of Dyez *et al.*, (2018) overlap PRED- CO_2 from ~1.38 – 1.5 Mya while the Chalk *et al.*, (2017) reconstruction
354 overlaps PRED- CO_2 from 1.09 – 1.43 Mya. Discrete reconstructions from Guillermic *et al.* (2022) are
355 distributed non-uniformly across the 800 to 1.5 Mya interval. For the two continuous $\delta^{11}\text{B}$ -based reconstructions
356 (Chalk *et al.*, (2017) and Dyez *et al.*, (2018)) the glacial CO_2 levels appear consistent with the PRED- CO_2
357 record, within their reported 30 – 60 ppm uncertainties. However, $\delta^{11}\text{B}$ -based interglacial stages in these
358 reconstructions exceed those of the PRED- CO_2 record (Fig. 4A). The Guillermic *et al.* (2022) reconstructions
359 suggest a larger range of CO_2 concentrations than the overlapping intervals of PRED- CO_2 and of the two
360 continuous $\delta^{11}\text{B}$ -based reconstructions (Fig. 4A). The large range of the Guillermic *et al.* (2022) data and the
361 high interglacial maxima in the Chalk *et al.* (2017) and Dyez *et al.*, (2018) data, all significantly exceed the
362 range and interglacial maxima from the BI- CO_2 estimates. These discrepancies internally between different
363 $\delta^{11}\text{B}$ -based CO_2 reconstructions and between the $\delta^{11}\text{B}$ -based reconstructions and the BI- CO_2 data, may be due to
364 uncertainties associated with the $\delta^{11}\text{B}$ proxy transfer function. The $\delta^{11}\text{B}$ -based CO_2 reconstructions are
365 dependent on assumptions about multiple components of the carbonate system, including local marine carbon
366 chemistry and the CO_2 saturation state in the past and (Hönisch *et al.*, 2009). Evidence that $\delta^{11}\text{B}$ -based
367 reconstructions may overestimate interglacial stage CO_2 is also seen in data from Chalk *et al.*, (2017) spanning
368 ca. 0–250 kya, where the $\delta^{11}\text{B}$ -based interglacial CO_2 levels exceed the continuous ice core CO_2 record by up to
369 ca. 30 ppm ~~(not shown)~~.

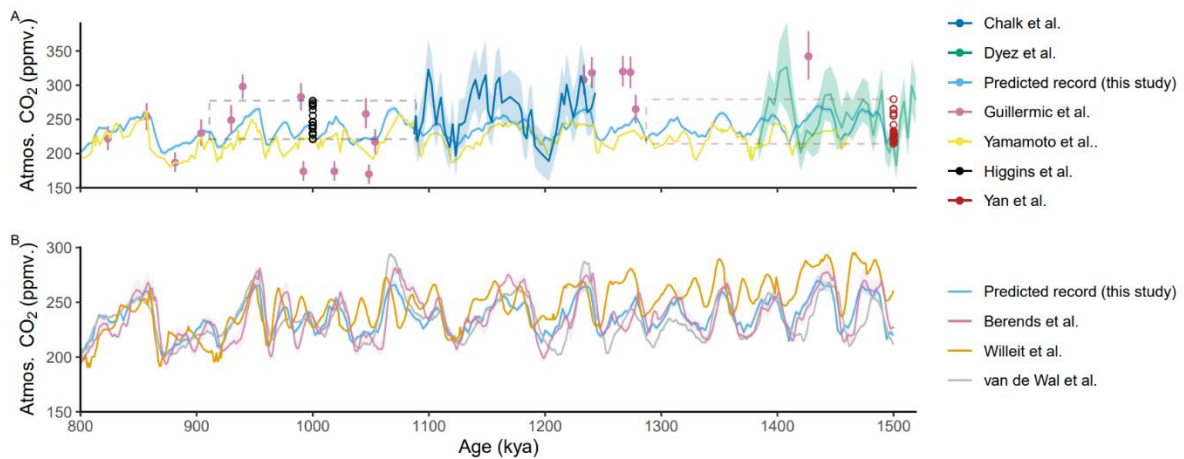
370

371 By comparison, the $\delta^{13}\text{C}$ of leaf wax data (Yamamoto *et al.*, 2022) has a similar glacial to interglacial range as
 372 PRED-CO₂, but a ca. 20ppm lower mean concentration than our predictions (Fig 4A). Hence, our PRED-CO₂
 373 data fall lower than interglacial $\delta^{13}\text{B}$ -based interglacial levels but are higher than the $\delta^{13}\text{C}$ of leaf-wax based
 374 estimate. The strong spread between these different proxies and the large associated uncertainty of the
 375 alternative marine and leaf wax proxy-CO₂ reconstructions mean that ~~Given the evidence that $\delta^{13}\text{B}$ -based~~
 376 ~~reconstructions are known to overestimate atmospheric CO₂ concentration in the continuous ice core record,~~ we
 377 do not find cause from the existing CO₂ proxy data to reject our predictions nor our associated null-hypothesis.
 378

379 We also compare our predictions to existing more complex model simulations (Fig 4B.). First, against a
 380 transient simulation using an intermediate-complexity earth system model (CLIMBER-2) by Willeit *et al.*
 381 (2019). This study suggests a combination of gradual regolith removal and atmospheric CO₂ decline can explain
 382 the long-term climate variability over the past 3_Myr. Second, against a longer-term reconstruction by van de
 383 Wal *et al.* (2011), which uses benthic $\delta^{18}\text{O}$ that utilises deep-sea benthic isotope records to reconstruct a
 384 continuous CO₂ record over the past 20 Myr. Third, a CO₂ reconstruction based on an inverse forward-
 385 modelling approach forced by a simple least-squares (LS) linear fit between the LR04 benthic stack, in which
 386 the forward model is and the current CO₂ ice core record, and incrementally updated through interaction with
 387 Global Circulation Model snapshots and the ANICE 3-D ice-sheet-shelf model (Berends *et al.* 2021ba). Our
 388 simple GLS model demonstrates a similar long-term trend and timing of glacial-interglacial signals and an
 389 atmospheric CO₂ level that sits approximately mid-way between the van de Wal *et al.* (2011), and Willeit *et al.*
 390 (2019) models and is remarkably similar to the Berends *et al.* (2021b) reconstruction, despite their different
 391 approach. Notably the Berends *et al.* reconstruction shows ~~Berends *et al.* reconstruction shows greater glacial~~
 392 to interglacial amplitude in the CO₂ signal compared to our GLS-model. The decreasing linear trend in CO₂ in
 393 Willeit *et al.* (2019), which is not seen in the other reconstructions, was directly prescribed in that study to
 394 induce Northern Hemisphere glaciation at 2.6 Myr ago. ~~The timing of the glacial cycles in our predictions~~
 395 match closely to those made by Berends *et al.* (2021a). ~~three other more complex models.~~
 396
 397
 398



399
 400



401

402 **Figure 4: A) Predicted CO₂ (this work) compared to observed, proxy CO₂ estimates from a range of other**
 403 **sources: $\delta^{11}\text{B}$ -based pCO₂ reconstructions and measurements by Dyez *et al.* (2018), Guillermic *et al.***
 404 **(2022); Chalk *et al.*, (2017); blue ice CO₂ measurements by Yan *et al.* (2019) and Higgins *et al.* (2015);**
 405 **$\delta^{13}\text{C}$ leaf wax proxy reconstructions by Yamamoto *et al.* (2022). The dashed boxes indicate the dating**
 406 **uncertainty and range of the respective BI-CO₂ records. B) Our predicted record compared to various**
 407 **model simulations: a regolith removal hypothesis simulation by Willeit *et al.* (2019); and [inverse-model](#)**
 408 **[based a high-resolution CO₂ reconstructions](#) by van de Wal *et al.* (2011), [and a least-squares linear](#)**
 409 **[regression based prediction](#) (Berends *et al.*, (2021ba)).**

410

411 A complete and critical test of our and other CO₂ predictions awaits the upcoming analysis of the continuous
 412 oldest ice core records. We now discuss some potential applications of the PRED-CO₂ record for hypothesis
 413 testing on the cause of the MPT.

414

415 PRED-CO₂ shows a long-term decline in glacial CO₂ across the MPT, but no long-term decrease in interglacial
 416 CO₂. This pattern is consistent with the boron-isotope-based CO₂ reconstructions shown earlier, where it is often
 417 described as an increase in the interglacial to glacial CO₂ difference (e.g., Chalk *et al.*, 2017; Hönlisch *et al.*,
 418 2009). Chalk *et al.*, (2017) concludes that the MPT was initiated by a change in ice sheet dynamics and that
 419 longer and higher-ice volume post-MPT ice ages are sustained by carbon cycle feedbacks, in particular dust
 420 fertilization of the Southern Ocean. That fact that our LR04-based prediction of CO₂ captures this same trend,
 421 **of declining glacial CO₂, with predicted glacial CO₂ fairly constant from 1.5 to ca. 1.0 Mya before declining**
 422 **from 1.0 to 0.6 kya,** reflects that LR04 benthic stack also features an increase in the interglacial to glacial
 423 benthic $\delta^{18}\text{O}$ difference across **this same interval-MPT**, which is dominated by the glacial **stage changes decline**
 424 (Fig 3A.). Here, a comparison of PRED-CO₂ to a realised continuous oldest ice core record will be of value.
 425 The agreement or disagreement would inform on the proportionality of the CO₂ coupling with ice volume; if
 426 there were a major new or non-linear process across the MPT that changed the nature of coupling between CO₂
 427 and ice volume the PRED-CO₂ and observed CO₂ records would be expected to diverge.

428

429 Another avenue to use the PRED-CO₂ record for hypothesis testing on the cause of the MPT concerns the phase
 430 locking hypothesis. The phase locking hypothesis is proposed to explain the absence of precession-related (23

431 kyr) periods in the LR04 benthic stack prior to the MPT (Fig 1), despite the strong precession cycle in insolation
432 (Raymo *et al.*, 2006, Morée *et al.*, 2021). The key concept is that prior to the MPT the Northern Hemisphere and
433 Antarctic ice sheets were responsive (in ice volume) to insolation changes in the precession band, but because
434 precession forcing is out of phase between the hemispheres, the ice volume changes were opposing between the
435 hemispheres and therefore cancelled in the benthic stack. This cancellation of the precession signal left
436 insolation forcing in the 41 kyr obliquity band to dominate globally integrated ice volume changes expressed in
437 the benthic stack. A transition from a smaller and more dynamic terrestrial-terminating Antarctic ice sheet to a
438 larger and more stable marine-terminating ice sheet with cooling climate across the MPT (e.g. Elderfield *et al.*,
439 2012) is then proposed to remove sensitivity of Antarctic ice volume to precession forcing and to suppress ice
440 sheet sensitivity to the obliquity band in favour of quasi-100kyr ice volume changes that are in phase between
441 the hemispheres (Raymo *et al.*, 2006).

442

443 Recently presented data from Yan *et al.* (2022), lend some support to the phase locking hypothesis, specifically
444 with evidence that pre-MPT Antarctic temperature (and by extension ice volume) is positively correlated with a
445 local precession-band insolation proxy based on the oxygen to nitrogen ratio of trapped air (Yan *et al.*, 2022).
446 Whereas the correlation becomes negative in the blue ice and continuous ice core data in the post-MPT record.
447 If Yan *et al.*, (2022) is correct and the phase locking hypothesis holds, then an implication is that prior to the
448 MPT, Antarctic climate, Antarctic ice volume and by extension Southern Ocean climate conditions, would fall
449 out of phase with the LR04 benthic stack. To now extend the argument to potential impacts on CO₂ exchange, if
450 the phase locking hypothesis holds, then prior to the MPT the Antarctic and Southern Ocean climate conditions
451 and by extension the Southern Ocean mechanisms of CO₂ exchange described earlier, would also be expected to
452 fall out of phase with the benthic stack. Since our regression model assumes continuation of the in-phase
453 relationship between the benthic stack and Antarctic and Southern Ocean climate conditions (as inherited from
454 the post-MPT training data) we would expect to see major disagreement between our pre-MPT CO₂ predictions
455 and a realised oldest ice continuous ice core CO₂ record.

456

457 **5 Summary and Conclusions**

458 In this study we have used a simple generalised least squares (GLS) model to predict atmospheric CO₂ from the
459 LR04 benthic $\delta^{18}\text{O}$ stack for the period spanning the mid-Pleistocene transition, 800–1500 kyr. Our CO₂
460 prediction is therefore based on the assumption that the physical processes linking CO₂, sea level, global ice
461 volume and ocean temperature over the past 800 kyr do not fundamentally change across the 800–1500 kya time
462 period. The null-hypothesis is deliberately simplistic on the basis that differences between our predictions and
463 observed or proxy CO₂ records may be revealing of the physical processes involved in the mid-Pleistocene
464 Transition.

465

466 We made initial tests of the null hypothesis by comparing our predicted CO₂ record to existing discrete blue ice
467 CO₂ records and other non-ice-core proxy-CO₂ records from the 800–1500 kyr interval. Our predicted CO₂
468 concentrations do not show any systematic departure from observed blue ice CO₂ concentrations. The
469 predictions are marginally lower (during glacial *and* interglacial stages) than those observed in blue ice from
470 1000 ± 89 kya and marginally higher than observed in blue ice data from $1.5 \text{ Mya} \pm 213$ kyr. Our predictions

471 were generally lower than interglacial $\delta^{11}\text{B}$ -based- CO_2 reconstructions, but higher than recent $\delta^{13}\text{C}$ of leaf-wax
472 based CO_2 reconstructions. Overall, we do not find clear evidence from the existing blue ice or proxy CO_2 data
473 to reject our predictions nor our associated null-hypothesis. The definitive test of our and other CO_2 predictions
474 therefore awaits the future analysis of the upcoming continuous oldest ice core records. The PRED- CO_2 record
475 presented here should provide a useful comparison to forthcoming oldest ice core records and opportunity to
476 provide further constraints on the processes involved in the MPT.

477

478 **Author contributions**

479 ~~Project design by JRWM, JBP and TRV. Data analysis and writing led by JRWM with contributions from all~~
480 ~~authors.~~ Project design by JBP, TRV and JRWM and supervision by TRV and JBP. Data analysis and figures
481 by JRWM with input from all authors. Writing led by JRMV and JBP. All authors contributed to and agreed on
482 the final version of the manuscript.

483

484 **Competing interests**

485 The authors declare that they have no competing interests.

486

487 **Disclaimer**

488 This study, to the best of the author(s) knowledge and belief, contains no material previously published or
489 written by another person, except where due reference is made in the text of the study.

490

491 **Acknowledgements**

492 We acknowledge assistance from Simon Wotherspoon (Institute for Marine and Antarctic Studies) in
493 appropriate model selection methods. This research was supported by the Australian Government through
494 Australian Antarctic Science projects 4632, the Million Year Ice Core (MYIC) Project and by the Australian
495 Government Department of Industry Science Energy and Resources, grant ASCI000002.

496

497 **Data availability**

498 PRED- CO_2 data ([0 to 1.5 Myr](#)) will be publicly archived at the Australian Antarctic Data Centre
499 (<https://data.aad.gov.au/> >>full link provided upon publication<<).

500

501 **References**

502 Archer, D., Winguth, A., D. Lea, and Mahowald, N.: What caused the glacial/interglacial atmospheric
503 pCO_2 cycle?, *Rev. Geophys.*, 38, 159–189, 2000, <https://doi.org/10.1029/1999RG000066>, 2000.

504

505 Bazin, L., Landais, A., Lemieux-Dudon, B., Toye Mahamadou Kele, H., Veres, D., Parrenin, F., Martinerie, P.,
506 Ritz, C., Capron, E., Lipenkov, V., Loutre, M.-F., Raynaud, D., Vinther, B., Svensson, A., Rasmussen, S.,
507 Severi, M., Blunier, T., Leuenberger, M., Fischer, H., Masson-Delmotte, V., Chappellaz, J., and Wolff, E.: An
508 optimized multi-proxies, multi-site Antarctic ice and gas orbital chronology (AICC2012): 120-800 ka, *Clim.*
509 *Past*, 9, 1715-1731, <https://doi.org/10.5194/cp-9-1715-2013>, 2013.

510

511 Bereiter, B., Eggleston, S., Schmitt, J., Nehrbass-Ahles, C., Stocker, T. F., Fischer, H., Kipfstuhl, S., and
512 Chappellaz, J.: Revision of the EPICA Dome C CO_2 record from 800 to 600 ky before present, *Geophys. Res.*
513 *Let.*, 42, 542-549, <https://doi.org/10.1002/2014gl061957>, 2015.

514

515 [Berends, C. J., Köhler, P., Lourens, L. J., and van de Wal, R. S. W.: On the cause of the mid-Pleistocene](#)
516 [transition., *Rev. Geophys.*, 59, e2020RG000727. <https://doi.org/10.1029/2020RG000727>, 2021a.](#)
517

518 Berends, C. J., de Boer, B., and van de Wal, R. S. W.: Reconstructing the evolution of ice sheets, sea level, and
519 atmospheric CO₂ during the past 3.6 million years. *Clim. Past*, 17, 361–377, [http://doi.org/10.5194/cp-17-361-](http://doi.org/10.5194/cp-17-361-2021)
520 [2021](#), 2021**ba**.
521

522 [Berends, C. J., Köhler, P., Lourens, L. J., and van de Wal, R. S. W.: On the cause of the mid-Pleistocene](#)
523 [transition., *Rev. Geophys.*, 59, e2020RG000727. <https://doi.org/10.1029/2020RG000727>, 2021b.](#)
524

525 Berger, A., Li, X. S., and Loutre, M. F.: Modelling northern hemisphere ice volume over the last 3Ma,
526 *Quaternary. Sci. Rev.*, 18, 1-11, [https://doi.org/10.1016/S0277-3791\(98\)00033-X](https://doi.org/10.1016/S0277-3791(98)00033-X), 1999.
527

528 Broecker, W.S.: Glacial to interglacial changes in ocean chemistry, *Prog. Oceanogr.*, 11 (2), 151-197.
529 [https://doi.org/10.1016/0079-6611\(82\)90007-6](https://doi.org/10.1016/0079-6611(82)90007-6), 1982.
530

531 Chalk, T., Hain, M., Foster, G., Rohling, E., Sexton, P., Badger, M., Cherry, S., Hasenfratz, A., Haug, G.,
532 Jaccard, S., Martínez-García, A., Pälike, H., Pancost, R., and Wilson, P.: Causes of ice age intensification across
533 the Mid-Pleistocene Transition. *P. Natl. Acad. Sci. USA.*, 114, 13114-13119,
534 <https://doi.org/10.1073/pnas.1702143114>, 2017.
535

536 Clark, P. U., Archer, D., Pollard, D., Blum, J. D., Rial, J. A., Brovkin, V., Mix, A. C., Pisias, N. G., and Roy,
537 M.: The middle Pleistocene transition: characteristics, mechanisms, and implications for long-term changes in
538 atmospheric pCO₂. *Quat. Sci. Rev.*, 25, 3150-3184, <https://doi.org/10.1016/j.quascirev.2006.07.008>, 2006.
539

540 Clark, P. U. and Pollard, D.: Origin of the Middle Pleistocene Transition by ice sheet erosion of regolith,
541 *Paleoceanography*, 13, 1-9, <https://doi.org/10.1029/97pa02660>, 1998.
542

543 Dyez, K.A., Hönisch, B., and Schmidt, G.A.: Early Pleistocene obliquity-scale pCO₂ variability at ~1.5 million
544 years ago. *Paleoceanogr. Paleoclimatol.*, 33, no. 11, 1270-1291, <https://doi.org/10.1029/2018PA003349>, 2018.
545

546 Elderfield, H., Ferretti, P., Greaves, S., Crowhurst, S., McCave, N., and Piotrowski, A.M.: Evolution of Ocean
547 Temperature and Ice Volume Through the Mid-Pleistocene Climate Transition, *Science*, 337,704-709,
548 <https://doi.org/10.1126/science.1221294>, 2012.
549

550 Gottschalk, J., Battaglia, G., Fischer, H., Frölicher, T.L., Jaccard, S.L., Jeltsch-Thömmes, A., Joos, F., Köhler,
551 P., Meissner, K.J., Menviel, L., Nehrbass-Ahles, C., Schmitt, J., Schmittner, A., Skinner, L.C., and Stocker,
552 T.G.: Mechanisms of millennial-scale atmospheric CO₂ change in numerical model simulations, *Quaternary.*
553 *Sci. Rev.*, 220, 30-74, <https://doi.org/10.1016/j.quascirev.2019.05.013>, 2019.
554

555 Guillermic, M., Misra, S., Eagle, R., and Tripathi, A.: Atmospheric CO₂ estimates for the Miocene to Pleistocene
556 based on foraminiferal δ¹¹B at Ocean Drilling Program Sites 806 and 807 in the Western Equatorial Pacific,
557 *Clim. Past*, 18(2), 183-207, <https://doi.org/10.5194/cp-18-183-2022>, 2022.
558

559 Hasenfratz, A. P., Jaccard, S. L., Martínez-García, A., Sigman, D. M., Hodell, D. A., Vance, D., Bernasconi, S.
560 M., Kleiven, H. F., Haumann, F. A., and Haug, G. H.: The residence time of Southern Ocean surface waters and
561 the 100,000-year ice age cycle, *Science*, 363, 1080, <https://doi.org/10.1126/science.aat7067>, 2019.
562

563 Higgins, J. A., Kurbatov, A. V., Spaulding, N. E., Brook, E., Introne, D. S., Chimiak, L. M., Yan, Y.,
564 Mayewski, P. A., and Bender, M. L.: Atmospheric composition 1 million years ago from blue ice in the Allan
565 Hills, Antarctica, *P. Natl. Acad. Sci. USA.*, 112, 6887, <https://doi.org/10.1073/pnas.1420232112>, 2015.
566

567 Hönisch, B., Hemming, N. G., Archer, D., Siddall, M., and McManus, J. F.: Atmospheric Carbon Dioxide
568 Concentration Across the Mid-Pleistocene Transition, *Science*, 324, 1551,
569 <https://doi.org/10.1126/science.1171477>, 2009.
570

571 [Huybers, P., & Wunsch, C. \(2005\). Obliquity pacing of the late Pleistocene glacial terminations. *Nature*,](#)
572 [434\(7032\), 491-494.](#)
573

574 International Panel on Climate Change: Climate change 2001; IPCC third assessment report, IPCC, Geneva,
575 2001.
576

577 International Partnerships in Ice Core Sciences: The oldest ice core: A 1.5 million year record of climate and
578 greenhouse gases from Antarctica [White paper]. [https://igbp-](https://igbp-scor.pages.unibe.ch/sites/default/files/download/docs/working_groups/ipics/white-papers/ipics_oldaa_final.pdf)
579 [scor.pages.unibe.ch/sites/default/files/download/docs/working_groups/ipics/white-papers/ipics_oldaa_final.pdf](https://igbp-scor.pages.unibe.ch/sites/default/files/download/docs/working_groups/ipics/white-papers/ipics_oldaa_final.pdf),
580 accessed 06/12/2023, 2020.
581

582 Jouzel, J., Masson-Delmotte, V., Cattani, O., Dreyfus, G., Falourd, S., Hoffmann, G., Minster, B., Nouet, J.,
583 Barnola, J. M., Chappellaz, J., Fischer, H., Gallet, J. C., Johnsen, S., Leuenberger, M., Loulergue, L., Luethi, D.,
584 Oerter, H., Parrenin, F., Raisbeck, G., Raynaud, D., Schilt, A., Schwander, J., Selmo, E., Souchez, R., Spahni,
585 R., Stauffer, B., Steffensen, J. P., Stenni, B., Stocker, T. F., Tison, J. L., Werner, M., and Wolff, E. W.: Orbital
586 and Millennial Antarctic Climate Variability over the Past 800,000 Years, *Science*, 317, 793,
587 <https://doi.org/10.1126/science.1141038>, 2007.
588

589 Lisiecki, L. E. and Raymo, M. E.: A Pliocene-Pleistocene stack of 57 globally distributed benthic $\delta^{18}\text{O}$ records,
590 *Paleoceanography*, 20, PA1003, <https://doi.org/10.1029/2004pa001071>, 2005.
591

592 Martínez-García, A., Sigman, D.M., Ren, H., Anderson, R.F., Straub, M., Hodell, D.A., Jaccard, S.L., Eglinton,
593 T.I., and Haug, G.H.: Iron fertilization of the subantarctic ocean during the last ice age, *Science*, 343 (6177),
594 1347-1350, <https://doi.org/10.1126/science.1246848>, 2014.
595

596 McClymont, E.L., Sostdian, S.M., and Rosell-Melé, A.: Pleistocene sea-surface temperature evolution: Early
597 cooling, delayed glacial intensification, and implications for the mid-Pleistocene transition. *Earth. Sci. Rev.*,
598 123, 173-193, <https://doi.org/10.1016/j.earscirev.2013.04.006>, 2013.
599

600 Millero, F. J.: Thermodynamics of the carbon dioxide system in the oceans, *Geochim. Cosmochim. Acta.*, 59,
601 661-677, [https://doi.org/10.1016/0016-7037\(94\)00354-O](https://doi.org/10.1016/0016-7037(94)00354-O), 1995.
602

603 Morée, A. L., Sun, T., Bretones, A., Straume, E. O., Nisancioglu, K., and Gebbie, G.: Cancellation of the
604 precessional cycle in $\delta^{18}\text{O}$ records during the Early Pleistocene. *Geophys. Res. Lett.*, 48,
605 e2020GL090035. <https://doi.org/10.1029/2020GL090035>, 2021.
606

607 Petit, J. R., Jouzel, J., Raynaud, D., Barkov, N. I., Barnola, J. M., Basile, I., Bender, M., Chappellaz, J., Davis,
608 M., Delaygue, G., Delmotte, M., Kotlyakov, V. M., Legrand, M., Lipenkov, V. Y., Lorius, C., Pépin, L., Ritz,
609 C., Saltzman, E., and Stievenard, M.: Climate and atmospheric history of the past 420,000 years from the
610 Vostok ice core, Antarctica, *Nature*, 399, 429-436, <https://doi.org/10.1038/20859>, 1999.
611

612 Raymo, M., Lisiecki, L., and Nisancioglu, K.: Plio-Pleistocene Ice Volume, Antarctic Climate, and the Global
613 18O Record, *Science*, 313, 492-495, <https://doi.org/10.1126/science.1123296>, 2006.
614

615 Raymo, M., Ruddiman, W., and Froelich, P.: Influence of Late Cenozoic mountain building on ocean
616 geochemical cycles, *Geology*, 16, 649-653, [https://doi.org/10.1130/0091-](https://doi.org/10.1130/0091-7613(1988)016<0649:IOLCMB>2.3.CO;2)
617 [7613\(1988\)016<0649:IOLCMB>2.3.CO;2](https://doi.org/10.1130/0091-7613(1988)016<0649:IOLCMB>2.3.CO;2), 1988.
618

619 Raymo, M. E.: The timing of major climate terminations, *Paleoceanography*, 12, 577-585,
620 <https://doi.org/10.1029/97PA01169>, 1997.
621

622 Raymo, M. E. and Huybers, P.: Unlocking the mysteries of the ice ages, *Nature*, 451, 284-285,
623 <https://doi.org/10.1038/nature06589>, 2008.
624

625 Röthlisberger, R., Bigler, M., Wolff, E. W., Joos, F., Monnin, E., and Hutterli, M. A.: Ice core evidence for the
626 extent of past atmospheric CO_2 change due to iron fertilisation, *Geophys. Res. Lett.*, 31, L16207,
627 <https://doi.org/10.1029/12004GL020338>, 2004.
628

629 Ruddiman, W. F., Raymo, M. E., Martinson, D. G., Clement, B. M., and Backman, J.: Pleistocene evolution:
630 Northern hemisphere ice sheets and North Atlantic Ocean, *Paleoceanography*, 4, 353-412,
631 <https://doi.org/10.1029/PA004i004p00353>, 1989.
632

633 Shackleton, N. J. and Pisias, N. G.: Atmospheric Carbon Dioxide, Orbital Forcing, and Climate. In: The Carbon
634 Cycle and Atmospheric CO₂: Natural Variations Archean to Present, <https://doi.org/10.1029/GM032p0303>,
635 1985.

636

637 Shugi, H., The older the ice, the better the science. *Adv. Polar Sci.*, 23, 121-122,
638 <https://doi.org/10.13679/j.advps.2022.0004>, 2022.

639

640 Stephens, B.B., Keeling, R.F.: The influence of Antarctic sea ice on glacial–interglacial CO₂ variations. *Nature*,
641 404, 171–174, <https://doi.org/10.1038/35004556>, 2000.

642

643 Tzedakis, P. C., Crucifix, M., Mitsui, T., and Wolff, E. W.: A simple rule to determine which insolation cycles
644 lead to interglacials, *Nature*, 542, 427-432, <https://doi.org/10.1038/nature21364>, 2017.

645

646 Ushie, H., and Matsumoto, K.: The role of shelf nutrients on glacial-interglacial CO₂: A negative
647 feedback, *Global Biogeochem. Cy.*, 26, GB2039, <https://doi.org/10.1029/2011GB004147>., 2012.

648

649 van de Wal, R. S. W., de Boer, B., Lourens, L. J., Köhler, P., and Bintanja, R.: Reconstruction of a continuous
650 high-resolution CO₂ record over the past 20 million years. *Clim. Past*, 7, 1459–1469. [https://doi.org/10.5194/cp-](https://doi.org/10.5194/cp-7-1459-2011)
651 [7-1459-2011](https://doi.org/10.5194/cp-7-1459-2011), 2011.

652

653 Veres, D., Bazin, L., Landais, A., Toyé Mahamadou Kele, H., Lemieux-Dudon, B., Parrenin, F., Martinerie, P.,
654 Blayo, E., Blunier, T., Capron, E., Chappellaz, J., Rasmussen, S., Severi, M., Svensson, A., Vinther, B., and
655 Wolff, E.: The Antarctic ice core chronology (AICC2012): an optimized multi-parameter and multi-site dating
656 approach for the last 120 thousand years, *Clim. Past*, 9, 1733-1748, <https://doi.org/10.5194/cp-9-1733-2013>,
657 2013.

658

659 Willeit, M., Ganopolski, A., Calov, R., and Brovkin, V.: Mid-Pleistocene transition in glacial cycles explained by
660 declining CO₂ and regolith removal, *Sci. Adv.*, 5, eaav7337, doi: 10.1126/sciadv.aav7337, 2019.

661

662 Wolff, E. W., Chappella, J., Fischer, H., Kull, C., Miller, H., Stocker, T. F., and Watson, A. J.: The EPICA
663 challenge to the Earth system modeling community, *EOS*, 85, 363363, <https://doi.org/10.1029/2004EO380003>,
664 2004.

665

666 Wolff, E. W., Kull, C., Chappellaz, J., Fischer, H., Miller, H., Stocker, T. F., Watson, A. J., Flower, B., Joos, F.,
667 Köhler, P., Matsumoto, K., Monnin, E., Mudelsee, M., Paillard, D., and Shackleton, N.: Modeling past
668 atmospheric CO₂: results of a challenge, *EOS*, 86 (38), 341-345, <http://doi.org/10.1029/2005EO380003>, 2005.

669

670 Yamamoto, M., Clemens, S.C., Seki, O., Tsuchiya, Y., Huang, Y., O’ishi, R., and Abe-Ouchi, A.: Increased
671 interglacial atmospheric CO₂ levels followed the mid-Pleistocene Transition, *Nat. Geosci.*, 15(4), 307–313,
672 <https://doi.org/10.1038/s41561-022-00918-1>, 2022.

673

674 Yan, Y., Bender M.I., Brook, E.J., Clifford, H.M., Kemeny, P.C., Kurbatov, A.V., Mackay, S., Mayewski,
675 P.A., Ng, J., Severinghaus J.P., and Higgins, J.A.: Two-million-year-old snapshots of atmospheric gases from
676 Antarctic ice, *Nature*, 574(7780), 663–666, <https://doi.org/10.1038/s41586-019-1692-3>, 2019.

677

678 Yan, Y., Kurbatov, A.V., Mayewski, P.A., Shackleton, S., and Higgins, J.A.: Early Pleistocene East Antarctic
679 temperature in phase with local insolation. *Nat. Geosci.*, 16, 50-55, [https://doi.org/10.1038/s41561-022-01095-](https://doi.org/10.1038/s41561-022-01095-x)
680 [x](https://doi.org/10.1038/s41561-022-01095-x), 2022.

681

682